Brief Report

DOI: 10.5582/irdr.2017.01065

# *In vivo* quantification of amyloid burden in TTR-related cardiac amyloidosis

**Alexander Marco Kollikowski[1,2,§], Florian Kahles[3,§], Svetlana Kintsler[4], Sandra Hamada[3], Sebastian Reith[3], Ruth Knüchel[4], Christoph Röcken[5], Felix Manuel Mottaghy[1,6,*], Nikolaus Marx[3], Mathias Burgmaier[3]**

[1] *Department of Nuclear Medicine, University Hospital RWTH Aachen, Aachen, Germany;*
[2] *Department of Neuroradiology, University Hospital of Würzburg, Würzburg, Germany;*
[3] *Department of Internal Medicine I – Cardiology, RWTH Aachen University, Germany;*
[4] *Department of Pathology, University Hospital RWTH Aachen, Aachen, Germany;*
[5] *Institute of Pathology, Christian-Albrechts-University and UKSH Campus, Kiel, Germany;*
[6] *Department of Radiology and Nuclear Medicine, Maastricht University Medical Center (MUMC), Maastricht, The Netherlands.*

**Summary** **Cardiac transthyretin-related (ATTR) amyloidosis is a severe cardiomyopathy for which therapeutic approaches are currently under development. Because non-invasive imaging techniques such as cardiac magnetic resonance imaging and echocardiography are non-specific, the diagnosis of ATTR amyloidosis is still based on myocardial biopsy. Thus, diagnosis of ATTR amyloidosis is difficult in patients refusing myocardial biopsy. Furthermore, myocardial biopsy does not allow 3D-mapping and quantification of myocardial ATTR amyloid. In this report we describe a $^{99m}$Tc-DPD-based molecular imaging technique for non-invasive single-step diagnosis, three-dimensional mapping and semiquantification of cardiac ATTR amyloidosis in a patient with suspected amyloid heart disease who initially rejected myocardial biopsy. This report underlines the clinical value of SPECT-based nuclear medicine imaging to enable non-invasive diagnosis of cardiac ATTR amyloidosis, particularly in patients rejecting biopsy.**

***Keywords:*** Cardiac ATTR amyloidosis, nuclear cardiac imaging, quantification, amyloid burden, myocardial biopsy, cardiac magnetic resonance imaging

## 1. Introduction

Cardiac transthyretin-related (ATTR) amyloidosis is a rare but severe form of restrictive cardiomyopathy, which is associated with clinical features of heart failure and adverse outcomes (*1*). Currently new promising therapeutic options based on pharmacological stabilization of tetrameric TTR are currently under development for the treatment of hereditary ATTR amyloidosis (*1,2*). However, ATTR amyloidosis is often challenging to diagnose, since non-invasive imaging techniques such as cardiac magnetic resonance imaging and echocardiography are non-specific. Thus, the diagnosis of ATTR amyloidosis is still based on myocardial biopsy, which is associated with a risk of several complications, including cardiac tamponade, myocardial perforation, hematoma, transient right bundle branch block, transient arrhythmias, tricuspid regurgitation, and occult pulmonary embolism (*3*). Moreover, myocardial biopsy does not allow a 3D-mapping and quantification of myocardial ATTR amyloid. Here we describe a $^{99m}$Tc-DPD-based molecular imaging technique for non-invasive single-step diagnosis, three-dimensional mapping and semiquantification of cardiac ATTR amyloid in a patient with suspected cardiac amyloidosis who initially rejected myocardial biopsy.

Released online in J-STAGE as advance publication November 27, 2017.

[§]These authors contributed equally to this work.

**Address correspondence to:*
Prof. Dr. Felix Manuel Mottaghy, Department of Nuclear Medicine, University Hospital RWTH Aachen, Pauwelsstr. 30, Aachen 52074, Germany.
E-mail: fmottaghy@ukaachen.de

## 2. Case Presentation

We report the case of a 76-year-old man who presented in 2016 with progressive dyspnea on exertion (New York Heart Association class III). The patient denied chest pain, syncope or palpitations. Furthermore, he reported a history of progressive sensorimotor polyneuropathy. Relevant coronary artery disease had previously been ruled out using coronary angiography. A 12-lead-ECG showed atrial fibrillation and low voltage (Figure 1A). Echocardiography revealed diastolic dysfunction with cardiac hypertrophy (septum thickness 15 mm) and preserved left ventricular ejection fraction. Consistent with heart failure with preserved ejection fraction (HFpEF), NT-proBNP levels were elevated (4,983 pg/mL). Contrast-enhanced cardiac magnetic resonance imaging (CMR) showed a ubiquitous subendocardial late gadolinium enhancement indicating cardiac storage disease (Figure 1B) and raised the suspicion of cardiac amyloidosis. Additional echocardiographic strain imaging demonstrated inhomogeneous strain patterns with reduced mid and basal myocardial longitudinal strain, whereas apical segments were unaffected (Figure 1C). Laboratory testing for sarcoidosis, hemochromatosis and monoclonal gammopathies proved negative. Because all diagnostic results showed classical - though unspecific - characteristics of cardiac ATTR amyloidosis, we planned myocardial biopsy to confirm the diagnosis. However, the patient rejected myocardial biopsy due to personal reasons.

In light of potential treatment options for ATTR amyloidosis with agents such as diflunisal or tafamidis (*1,2*), we were challenged using a non-invasive technique 1. to confirm the diagnosis of cardiac ATTR amyloidosis and 2. to quantify disease severity and clinical relevance for the patient.

## 3. Results and Discussion

### 3.1. *Non-invasive diagnosis of cardiac ATTR amyloidosis*

Gillmore and colleagues reported recently that $^{99m}$Technetium-3,3-diphosphono-1,2-propanodicarboxylic acid ($^{99m}$Tc-DPD) could be used to diagnose cardiac ATTR amyloidosis with excellent sensitivity (> 99%) and high specificity (~86%) (*4*). Although the exact mechanism is not completely understood, $^{99m}$Tc-DPD shows highly preferential, potentially calcium-dependent, uptake in myocardial amyloid infiltrations caused by extracellular deposits of destabilized and dissociated TTR-tetramers which form fibrils consisting of misfolded TTR-subunits in a cross β-sheet structure (*1,5*).

In our patient, we performed a dual-phase bone scintigraphy after injection of 705 MBq $^{99m}$Tc-DPD using a dual-head system for image acquisition (ECAM, Siemens Healthcare, Erlangen, Germany). Whole body scans were obtained at 5 min and 3 h p.i. revealing inhomogeneous cardiac uptake (Figure 2). Considering the patient's symptoms, clinical history and previous diagnostic steps, the criteria for non-invasive diagnosis of ATTR amyloidosis proposed by Gillmore and colleagues were fulfilled (*4*).

### 3.2. *Quantification and 3D-mapping of cardiac ATTR amyloidosis*

Quantification of myocardial disease severity is important to determine clinical relevance of disease and treatment success of emerging therapeutic strategies for cardiac ATTR amyloidosis. However, quantification and 3D-mapping of cardiac ATTR amyloidosis using $^{99m}$Tc-DPD apart from visual assessment of planar images or heart-to-contralateral ratio is unknown (*5*).

First, we performed 3D-mapping of cardiac amyloid deposits and performed single photon emission computed tomography (SPECT, Symbia, Siemens Healthcare, Erlangen, Germany) 3.5 h p.i., which showed inhomogeneous tracer distribution within the heart with relative tracer absence in the apex, apical and mid-cavitary anterolateral wall, whereas the remaining myocardium revealed avid $^{99m}$Tc-DPD uptake (Figure

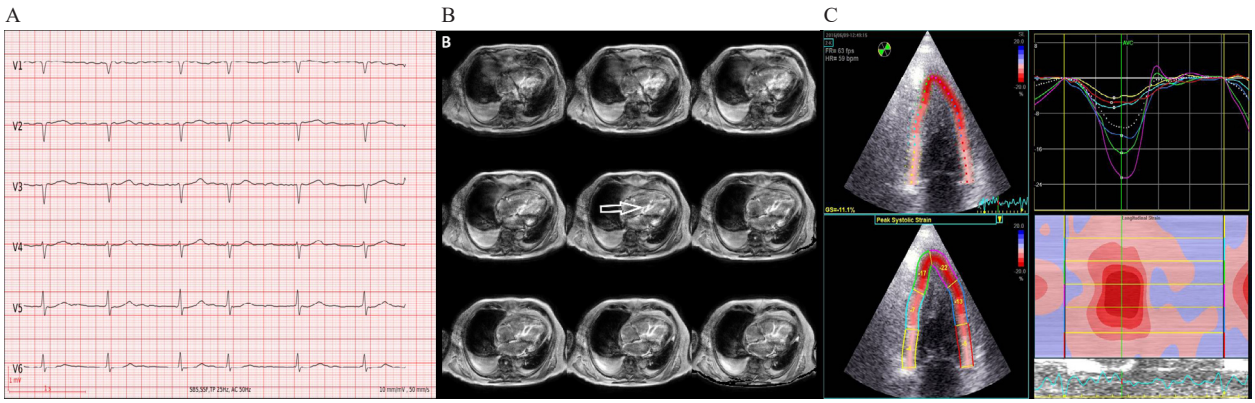


**Figure 1. (A), 12 lead ECG revealing atrial fibrillation and low voltage. (B), Late gadolinium enhancement (LGE) Inversion Recovery-Sequence (4-chamber-view), showing subendocardial to diffuse intramyocardial LGE. (C), 2D strain analysis of a 2 chamber-view showing preserved longitudinal strain of the apical LV-segments in contrast to the impaired longitudinal strain of the medial and basal LV-segments ("apical sparing").**

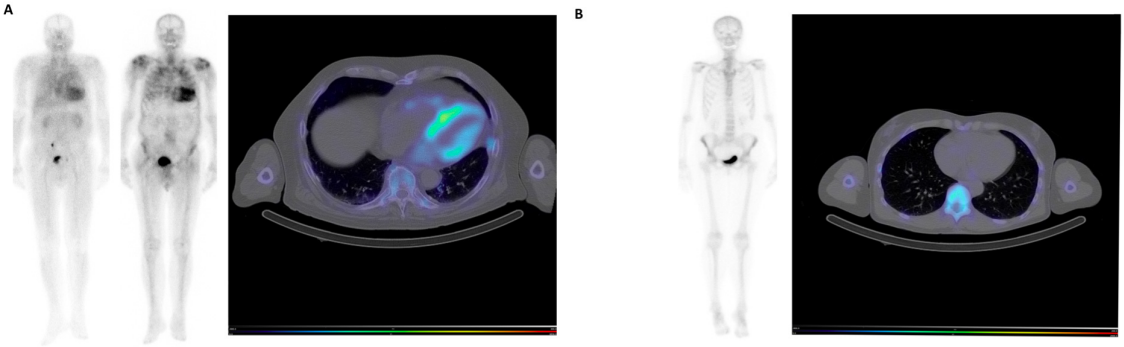


**Figure 2. (A), *Left:* Whole body scans 5 min and 3 h p.i. showing inhomogeneous cardiac $^{99m}$Tc-DPD retention. *Right section*: Cardiac SPECT/CT 3,5 h p.i. with regionally variable tracer distribution and relative tracer absence in the apex and mid-cavitary anterolateral wall. (B), $^{99m}$Tc-DPD scan in a control patient on the same day. Neither analogous planar imaging 3 h p.i. nor SPECT/CT 3,5 h p.i. reveales cardiac tracer uptake.**

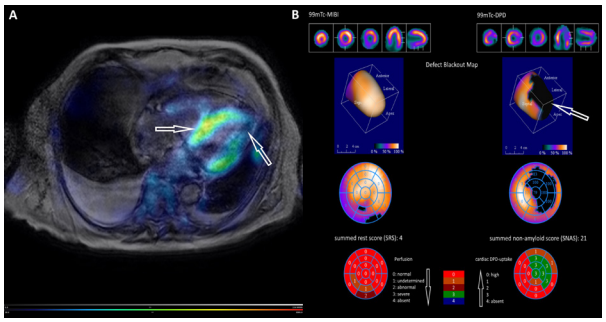


**Figure 3. (A), Fusion of SPECT dataset 3,5 h p.i. and CMR (Inversion Recovery-Sequence, 4-chamber-view) in corresponding axial alignment demonstrates congruent $^{99m}$Tc-DPD uptake and LGE with unaffected apical segments. (B), Nuclear cardiac imaging using a multi-detector SPECT system.** *Left*: $^{99m}$Tc-sestamibi scans (cationic complex exclusively characterizing unscathed mitochondria and vital cardiomyocytes), rest-only myocardial perfusion examination. *Upper row*: The summary screen of the main cardiac axes outlines no significant perfusion defects under resting conditions. *Middle*: 3- and 2-dimensional polar mapping. No significantly impaired left ventricular tracer uptake compared to the reference database ($^{99m}$Tc-sestamibi). Depiction as Defect Blackout Map. *Bottom row*: SRS ("Summed Rest Score"), semiquantitatively reflecting the extent of the perfusion defect (SRS ≤ 4 was regarded as normal). *Right*: $^{99m}$Tc-DPD scans 4 h p.i.. Tracer uptake in areas of presumed TTR-deposits. Upper row: The summary screen shows left ventricular $^{99m}$Tc-DPD defects in the apex and mid-cavitary anterolateral wall. *Middle*: The 3- and 2-dimensional Defect Blackout Maps show a significantly impaired apical and mid-cavitary anterolateral tracer uptake (reference database $^{99m}$Tc-sestamibi), which was regarded as unaffected myocardium. *Bottom row*: SNAS ("Summed Mon-Amyloid Score"), semiquantitatively reflecting the extent of suspected TTR-free myocardium.

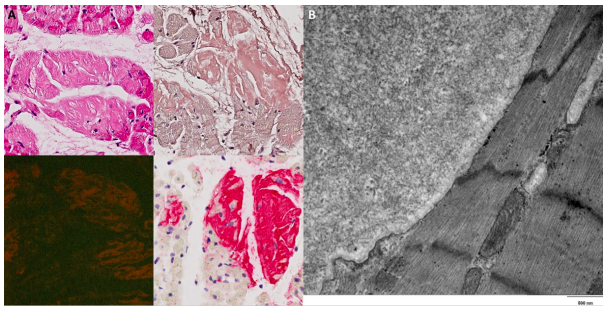


**Figure 4. (A), Histology of cardiac biopsy.** At the top on the left: eosinophilic deposits, hematoxylin and eosin stain (H&E), ×400 magnification. At the top on the right: acellular amorphic deposits, Congo red stain, ×400 magnification. At the bottom on the left: typical fluorescence signal of amyloid in a Congo red stained section viewed by fluorescence microscopy, ×200 magnification. At the bottom on the right: strong immunostaining of the amyloid deposits with an anti-transthyretin-antibody, ×400 magnification. **(B), Ultrastructural analysis of the cardiac biopsy by electron microscopy reveals the presence of irregular formed fibres.**

2). Then, SPECT and CMR data were merged into one image and both showed identical diseased and healthy segments of the heart (Figure 3A), suggesting that the late gadolinium enhancement observed in CMR could be explained by amyloid deposits.

For direct quantification of cardiac ATTR amyloidosis, we applied a method analogous to the well-established and validated techniques used in myocardial perfusion SPECT (*6*): A multi-detector SPECT system (Discovery NM 530c, GE Healthcare, Chicago, Illinois, USA) optimized for cardiac imaging and photon energy ranges between 40-200keV ($^{99m}$Tc: 140keV) was utilized to obtain $^{99m}$Tc-DPD scans 4 h p.i. (Figure 3B, right section). Additional myocardial perfusion SPECT (7-day time interval) after injection of 388 MBq $^{99m}$Tc-sestamibi were used to quantify viable myocardium and revealed no significant perfusion defects under resting conditions (Figure 3B, left section). Semiquantitative analysis of myocardial perfusion and left ventricular amyloid were assessed using polar mapping (Figure 3B, middle), a three- or two-dimensional (voxel- or pixel-based) depiction of the study's normalized cardiac activity counts compared with a reference database ($^{99m}$Tc-sestamibi) and followed by blacking out regions below a defined threshold of database activity (Defect Blackout Map). For additional semiquantitative scoring of myocardial perfusion defects or amyloid deposits, polar maps comprising 17 segments were generated, each of which was assessed separately with a score between 0 (i.e. no deviation between database and study) and 4 (i.e. significant deviation) (Figure 3B, bottom row). Concerning myocardial perfusion under resting conditions, the total score is referred to as "summed rest score" (SRS),

which, inter alia, reflects areas of myocardial scar tissue (*6*). Finally, to quantify left ventricular ATTR amyloid burden, we propose to introduce a reciprocal "summed non-amyloid score" (SNAS), which presumably reflects the extent of unaffected myocardium. Its theoretical range extends from SNAS = 0, *i.e*. massive $^{99m}$Tc-DPD uptake reflecting a homogeneously affected left ventricle, to SNAS = 68, *i.e*. no $^{99m}$Tc-DPD uptake and therefore no detectable cardiac ATTR amyloidosis.

3.3. *Myocardial biopsy confirmed imaging diagnosis*

On the basis of these new results, the patient gave informed consent to undertake myocardial biopsy. Ultrastructural analysis by electron microscopy revealed the presence of irregular formed fibrils and large deposits of amyloid were found in Congo red stained tissue sections showing a typical green birefringence under polarized light and a characteristic fluorescence signal in fluorescence microscopy (Figure 4). The amyloid deposits were immunostained with an antibody directed against transthyretin (Figure 4A). No immunostaining was found with antibodies directed against lambda- and kappa light chain (not shown). Later genotyping subclassified wild-type ATTR amyloidosis, as a consequence the patient was referred to a specialized center to assess further treatment options.

## 4. Conclusion

In this work we describe a $^{99m}$Tc-DPD-based molecular imaging approach for non-invasive diagnosis and semiquantification of cardiac ATTR amyloidosis in a patient with suspected cardiac amyloidosis who initially rejected myocardial biopsy. Due to promising new therapy options for hereditary ATTR amyloidosis based on pharmacological stabilization of tetrameric TTR such as diflunisal and tafamidis (*1,2*), imaging is not only crucial for a non-invasive diagnosis and early therapy planning in patients who refuse myocardial biopsy, but also regarding disease monitoring and response to therapy.

Our report stresses the clinical value of $^{99m}$Tc-DPD-based nuclear medicine imaging to provide a quick and accurate diagnosis of cardiac ATTR amyloidosis, particularly in patients refusing biopsy. Furthermore, we describe for the first time a widely available SPECT-based technique for single-step diagnosis, three-dimensional mapping and semiquantification of cardiac ATTR amyloidosis. Future studies are warranted to evaluate the suitability of $^{99m}$Tc-DPD-based quantification of myocardial ATTR amyloidosis for disease monitoring and its response to medical therapy.

## References

1. Ruberg FL, Berk JL. Transthyretin (TTR) cardiac amyloidosis. Circulation. 2012; 126:1286-1300.
2. Maurer MS, Grogan DR, Judge DP, Mundayat R, Packman J, Lombardo I, Quyyumi AA, Aarts J, Falk RH. Tafamidis in transthyretin amyloid cardiomyopathy: Effects on transthyretin stabilization and clinical outcomes. Circ Heart Fail. 2015; 8:519-526.
3. From AM, Maleszewski JJ, Rihal CS. Current status of endomyocardial biopsy. Mayo Clin Proc. 2011; 86:1095-1102.
4. Gillmore JD, Maurer MS, Falk RH, *et al*. Nonbiopsy diagnosis of cardiac transthyretin amyloidosis. Circulation. 2016; 133:2404-2412.
5. Narotsky DL, Castano A, Weinsaft JW, Bokhari S, Maurer MS. Wild-type transthyretin cardiac amyloidosis: Novel insights from advanced imaging. Can J Cardiol. 2016; 32:1166.e1-1166.e10.
6. Verberne HJ, Acampa W, Anagnostopoulos C, *et al*. EANM procedural guidelines for radionuclide myocardial perfusion imaging with SPECT and SPECT/CT: 2015 revision. Eur J Nucl Med Mol Imaging. 2015; 42:1929-1940.

*(Received September 28, 2017; Revised November 1, 2017; Accepted November 13, 2017)*